


Comparative evaluation of aircraft joint stiffness between intermediate and high level of detail models

Marco Tulio dos Santos¹ and Marcelo Greco^{1*} 

¹Programa de Pós-Graduação em Engenharia de Estruturas, Universidade Federal de Minas Gerais, Av. Antônio Carlos, 6627, Pampulha, 31270-901, Belo Horizonte, Minas Gerais, Brazil. *Author for correspondence. Email: mgreco@dees.ufmg.br

ABSTRACT. The present work aims to compare results in aircraft joints, focusing on spar and skin regions, considering two levels of detail to understand the differences in the structural response using different types of modeling (numerical and semi-analytical Rutman approach). Several studies were already performed to obtain the correct understanding of how actual loads are distributed through the joints. Finite Element Analysis modeling made using Nastran software were performed here. The study has shown the differences between the models analyzed by comparing the stiffness of the fasteners at the specific region analyzed. Results indicate good agreement between models for translational stiffness and more significant differences for rotational stiffness. The finite elements model with high level of detail presents larger rotational stiffness when compared with the Rutman approach.

Keywords: hierarchical models; aircraft joints; finite element methods; aircraft fasteners.

Received on September 4, 2023.
Accepted on April 11 2024.

Introduction

The procedure to build a new aircraft lies in a long-term product development cycle. A great amount of the resource and time is consumed during the execution process and the load distribution through the parts must be calculated. Moreover, the dimension of the components and all the needed specifications to comply with the regulator agency requirements must be defined. Basically, a commercial aircraft is lifted by its wing, while the fuselage is responsible to carry the payload and the empennage is responsible to stabilize the load distribution during the flight. Hence, the main load of an aircraft flows from the wings to the fuselage and the components used to build these parts and to connect them must be able to withstand this flow of load. Moreover, an aircraft is composed of hundreds of parts and thousands of fasteners are used to connect them.

The structural sizing of an aircraft component also involves the execution process, in which it is required from the team a high efficiency, quality and assertiveness in the response. Several parts of the aircraft must be sized by means of a high interaction of different technology and they must specify the dimensions, material, heat treatment, fasteners and several characteristics that will define the capability of the component to withstand all flight conditions envelope and its applicable safety factor which was already defined by the requirements. Mathematical tools can be used to support the engineering in such a task, as the Finite element Method for instance. But the choice of the method alone is not enough to correctly obtain the strain field of a component. It is also necessary to define the level of detail to be used to obtain satisfactory results.

Several authors have already studied the best way to obtain the load distribution in aircraft joints, both homogeneous and hybrid (when used composite parts connect to metallic). Santos, de Sá Martins, and Greco (2021) have proposed complete way to define the joint connections and its translational or rotational stiffness. Additionally, the authors have studied the impact and differences in using different methods to calculate joint stiffness and the effect of the secondary bending in those joints. In contrast to detailed models which demand a high computational cost and a great amount of time, there are models with low level of detail to represent joints that, however, offer accurate and trustworthy results.

Chaves and Fernandes (2016) have discussed aircraft joints and there, it is presented many types of aircraft joints, its capabilities, its particularities and how the load are distributed and transferred throughout the parts connected. During the process of sizing the aircraft joints, some failure modes must be considered. As it was discussed by Chaves and Fernandes (2016) the failure modes related to a shear joint.

In a joint with several rows, the load transferred for each fastener is known as bearing load, and the load that remains in the plate is called bypass load. Some authors, such as Niu (2011), already proposed a way to provide the load distribution by means of determination of the joint flexibility.

Rivet joint procedure are very complex and depend on the integrated effect of many variables related to joint design, production, and applied load condition. Most of the aircraft joints are assembled with rivets, which is easier to assemble and disassemble. Furthermore, some specific methods of connection can be considered, like the insertion of adhesive in riveting joint, already discussed by Sadowski, Balawender, Śliwa, Golewski, and Kneć (2013). In this study authors compare three types of configurations: spot welding plus adhesive, rivet bonded and clinch bonded joints. It is also possible to observe the positive effect of applying adhesive that makes the joint stronger and with better fatigue properties, better corrosion resistance and the possibility to remove the sealing in operation process.

Another interesting study was proposed by Huskamuri and Lagdive (2017), which aims to simulate the load transferred between the fasteners by using a 3D ANSYS model. In this study the numerical results have shown that less conservative and more accurate studies must be performed to achieve better results. Huan and Liu (2017) simulate three levels of force to evaluate the influence of this force in static behavior. Finally, the study conclude that the squeeze force does not have influence in joint stiffness, but results in a slight decrease in joint strength and the great squeeze force.

Skorupa, Machniewicz, Korbel, and Skorupa (2010) also point out the relevance of the secondary bending in rivet lap joint, specially related to fatigue life. This effect occurs due to an eccentricity at the joint and can be assumed as the responsible for the crack nucleation at the rivet hole region, causing a crack propagation that will cause a catastrophic failure if not identified in time. The authors have shown that the effect of secondary bending can be accounted by using differential equation, although this simplification is not able to predict this stress for thinner sheet and as a conclusion it is shown the nonlinear behavior of secondary bending, in which it can be decreased by increasing the pitch of fasteners or decreasing the thickness of the plate.

Thus, the load distribution in a joint can be influenced by several factors like materials properties, squeeze force, thickness of the plates attached, among others. The best way to simulate the load transferred in a joint using finite element approach is by using a higher order solid element, considering the nonlinearities of material, the geometry and the contact between the parts.

In hierarchical model point of view, the abstraction of using a high complex nonlinear model refers to a more representative model, which has a high level of detail but is difficult to execute in practice. In a full model of a wing, with thousands of rivets used to attach spars with skins and rib with skins. This is not feasible in practice, not only due to hardware limitation, but also due to the product cycle deadline. Because of such complexity, some intermediates models are proposed to accelerate the process of sizing a complex component with several attachment regions, but even so using an assertive approach.

Askri, Bois, and Wagnier (2016) has proposed a reduced model by using Multi-Connected Rigid Surface (MCRS) to predict the stress field at local region of the fastener and to predict the load distribution in fasteners. In this model, also called MCRS, the authors have included the effect of pre-load and friction coefficient and the conclusions have very satisfactory results, not only for global stiffness and the distribution of load between fasteners, but also for local response assessed from contact pressure and stress fields. Askri, Bois, and Wagnier (2016) have proposed a study to investigate the effect of hole location error on the strength of fastened multi-material joint, using the same approach (MCRS), and the study was performed considering statistical approaches. This work shows the link between the transmitter load with the bolt-hole clearance. Askri, Bois, and Danoun (2021), by exploring the same methodology of MCRS, have proposed another study to investigate the effect of shape defect in multi-fastened joint during the assembly process. The numerical model previously proposed has shown the ability to simulate different clamp sequences and to capture the interaction between shape effects, bolt-hole clearance and target axial pre-load. However, the success in the results for the model proposed is limited to its specific applicability and for each specific situation new models must be considered.

Gray and McCarthy (2011) have proposed a combination of analytical and numerical approaches to simulate a bolted composite joint. A semi-empirical approach for model failure initiation and energy absorption is used. An element is proposed in which it can represent the nonlinearities, load-displacement behavior of composite joint, ranging from bolt-hole clearance and friction effect to eventual joint failure. The authors have concluded that the model proposed is robust and presented a good correlation with the actual model; besides, the model has shown the capability to capture complex load distribution for more than twenty bolts.

In 2015, by testing a series of single bolt joints with various bolt-holes clearances and bolt tightening torques to confirm the influence coefficient of the joint stiffness model, Liu, Zhang, Zhao, Xin, and Zhou (2015) have presented a good correlation with the experimental tests. Furthermore, the study has proposed a joint stiffness model. Another interesting point observed by Liu et al. (2015) is the influence of the friction in load transference: it is proved that when it is applied a great torque, the bolt starts to transfer the load only after the frictional load be overcome. It is also showed that for fasteners finger-tight there is almost zero frictional load, and the load is transferred only by the fasteners.

Liu et al. (2020) have continued the study and have proposed an improved 2D finite element model for bolt load distribution analysis of composite multi-bolt single-lap joints. The authors use 2D finite element to simulate a single lap joint and uses a 3D model to validate the results. Liu et al. (2020) have simulated HST10-10 bolt and uses ABAQUS techniques to calculate the bolts by an improvement of the technique proposed by Liu et al. (2020). Besides, the load displacement curve was replaced by the bolt stiffness model already proposed (Liu et al., 2015). Furthermore, bolt holes are added in the model, taking the area of bolt head as the size of influence region of coupling constraints. The authors have concluded that there is no significant influence in change simulation approaches of the bolt-stiffness from load-displacement. Besides, the bolt holes influences the accuracy of the calculation, but the area of influence region has no effect on the load distribution, although it influences in predicting the secondary bending effect.

Another interesting study was proposed by Huskamuri and Lagdive (2017), which aims to simulate the load transferred between the fasteners by using a 3D ANSYS model. In this study the numerical results have shown not conservative and more accurate studies must be performed to achieve better results.

Verwaerde, Guidault, and Boucard (2021) use a non-linear connector to simulate the behavior of bolt assembly and bolt pre-load, friction and plastic material parameters. The connection is implemented using ABAQUS through user-element subroutine and the result is compared with large scale 3D calculation, which has presented a good correlation, but the reduced model has cpu time reducing compared with 3D model.

Santos et al. (2021) have presented the variability of the load distribution in joints by considering different types of approaches. In the study, the authors have compared results for experimental tests and numerical simulation for joints modeled with different techniques which range from the simplest to the most complex. Santos, Sá Martins, and Greco (2021) present a comparative study between aircraft joints, considering three different levels of FEM models fidelity.

As observed in the proposed studies, the most accurate method to mathematically obtain the joint stiffness is through a complex nonlinear solid model. Thus, present work uses a model with high level of detail to represent the joint region considering geometrical, material and contact nonlinearities to perform the analysis. The work focuses the effort in understand the impact in change the level of detail of a mathematical model used to simulate a region of an aircraft wing under a hypothetical flight load.

Material and methods

Wing structure model

Structural analysis of a wing is considered here, considering load distribution along the wing spanwise and how this load flow through one component to another such as spar to skin and skin to rib. To simplify the analysis and make possible to focus on what is really relevant for the study proposed, a wing box with two spars attached to the skin and some ribs distributed equally spaced along the spanwise are going to be simulated (Santos et al., 2021). The attachment between skin and spar, wing trailing and leading edges were not considered in the model. The wing, ribs and spars are supposed to be built by 7475-T761 aluminum, and its properties are provided by Niu (2011). the thickness of the components are presented in Table 1 and the overview of the wing studied is presented in Figure 1.

Table 1. Components and thickness of the wing analyzed.

Component	Thickness [mm]	Material
Skin	3.00	7475- T761
Skin reinforcement	3.75	
Ribs	3.00	
Spars	4.50	

The fastener used to accomplish the attachment is going to be HST-10, made of titanium. Its properties are shown on Table 2.

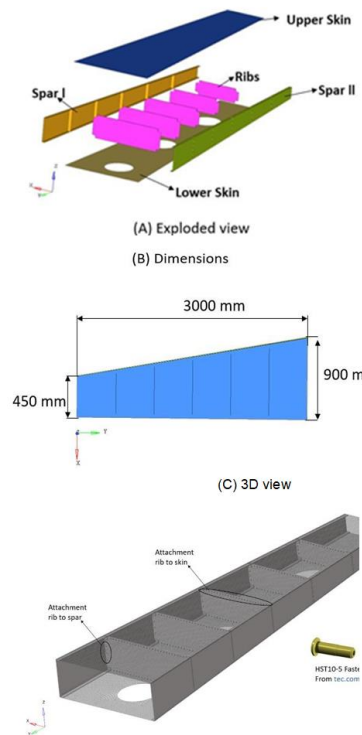


Figure 1. Wing overview and dimensions. Adapted from: Santos et al. (2021).

Table 2. Fasteners used.

Fastener	Diameter [mm]	Material
HST10-5	3.97	Titanium

The attachment between the ribs and spars and between the ribs and skins is going to be a shear joint with a single row and with at least 3 times the diameter of the fasteners for the distance between the fasteners and 2 times the diameter for the distance between the center of the hole and the edge.

Considering two levels of modelling approach, the purpose is to investigate the behavior of the stiffness and the load distribution throughout the attachment region between the spar and skin in an aircraft wing under flight loads. The models described are discretized in two different levels of detail to compare the results. The first one is going to be the less representative, while the second will be the one with more detail to represent the actual structure and it will be used as the reference to compare the results.

Intermediate level of detail

For this model, all components (spar, skin and ribs), including its reinforcements are going to be modeled considering shell elements with serendipity formulation. The fasteners are going to be modeled using the Rutman approach (Santos et al., 2021), and according to the method, two kinds of stiffness — translational and rotational — must be calculated in the region where the fastener touches the plate and those values must be assigned to the bush. The value for translational stiffness is calculated based on Equation 1, whereas the rotational stiffness is calculated based on Equation 2. The values of this stiffness calculated for each region are presented in Table 3.

$$S_{bt_i} = \frac{t_{pi}}{\frac{1}{E_{cp}} + \frac{1}{E_{cf}}} \quad (1)$$

$$S_{br_i} = \frac{t_{pi}^3}{12 \left(\frac{1}{E_{cp}} + \frac{1}{E_{cf}} \right)} \quad (2)$$

where E_{cp} is the compression modulus of plate i material, E_{cf} is the compression modulus of fastener material and t_{pi} is the thickness of plate i .

Most of the elements are going to be QUAD4, but in some regions TRIA3 was necessary. Figure 2 shows the representation of spar, skin, and ribs. The average size of the elements is 30mm and Figure 3 presents the FEM joint detail for this model.

Table 3. Joints properties.

Component	Thickness [daN mm ⁻²]	E_{cp} [daN mm ⁻²]	E_{fp} [daN mm ⁻²]
Upper skin	3	7100	11400
Lower skin	3	7100	11400
Reinforcement upper skin	3.75	7100	11400
Reinforcement lower skin	3.75	7100	11400
Ribs	3	7100	11400
Spar left side	4.5	7100	11400
Spar right side	4.5	7100	11400

Component	Translational stiffness [daN mm ⁻¹]	Rotational stiffness [daN mm rad ⁻¹]
Upper skin	13125.41	9844.05
Lower skin	13125.41	9844.05
Reinforcement upper skin	16406.76	19226.67
Reinforcement lower skin	16406.76	19226.67
Ribs	13125.41	9844.05
Spar left side	19688.11	33223.68
Spar right side	19688.11	33223.68

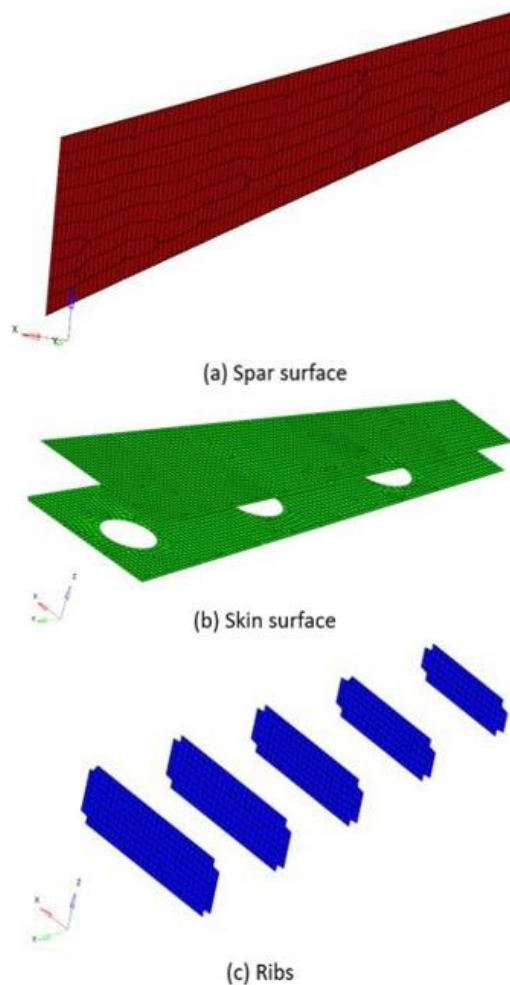


Figure 2. Shell elements for Model 1.

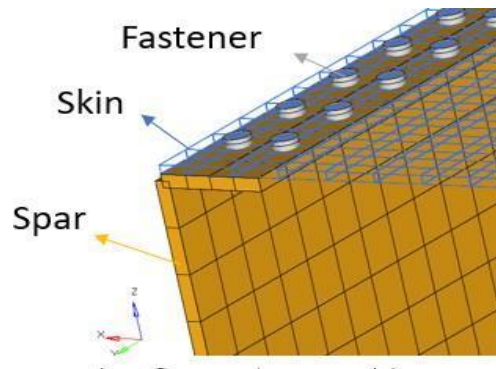


Figure 3. Model with intermediate level of detail. Adapted from: Santos et al. (2021).

High level of detail

The model with high level of detail is the most complex of them in a numerical point of view, since it is using more complex elements with more complex function of shape, besides the nonlinearities which were considered. Most of the elements used are CHEXA with 8 nodes, but when this is not possible, CPENTA elements with 6 nodes are used. Unlike the first, this model does not use simplifications to simulate the connections, it uses Finite Element Approach in order to simulate all parts and behavior of the connection. Another important difference in this model, when compared to the other simplification, is that only a portion of the wing is going to be built, since it should be impracticable to work with the whole model considering this level of detail.

The region chosen to be portioned will be the one that presents the higher flow of load along the wing spanwise. As it can be seen in Figure 4, the critical region is located near the root of the wing and, therefore, close to the first rib. This is an expected behavior since there is an increase in wing stiffness in rib region and consequently an increase in flow of load. The model is discretized according to the approach proposed. Nonlinearities of the material, large displacement and contact nonlinearities are considered. No gap between the plates is considered.

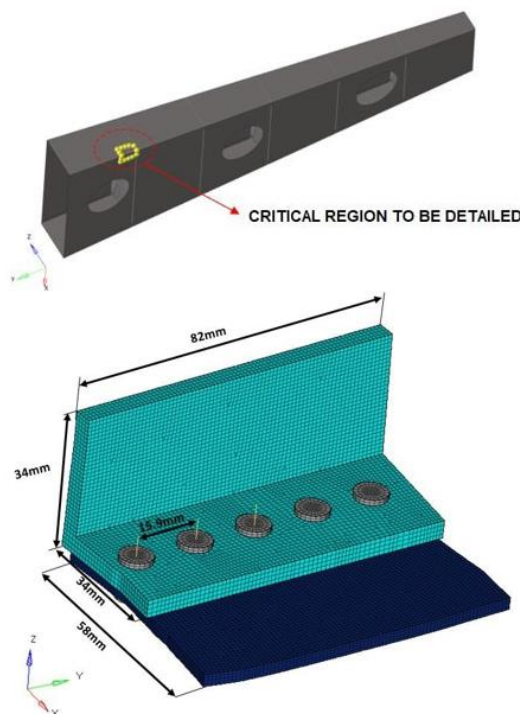


Figure 4. Region chosen to be detailed with a single shear joint.

Initial conditions

The load distribution was done in such a way as the total load equals 4000 daN. The aerodynamic moment (considered being at 1/4 of the chord) was calculated based on Abbott and von Doenhoff (2012).

$$L = \frac{1}{2} \rho V^2 S_w C_L, \quad (3)$$

$$M_x = \frac{1}{2} \rho V^2 S_w \bar{c} C_m = \frac{C_m}{C_L} L \bar{c} \quad (4)$$

where: L is the lift; M_x is the moment; ρ is the air density; V is the reference speed; S_w is the plain view wing area; \bar{c} is the mean aerodynamic chord, in this case it is 700 mm; C_m is the moment coefficient; C_L is the lift coefficient.

Considering the profile NACA 006 (Abbott & von Doenhoff, 2012), with the angle of attach equal to 0, the C_m value is -0.2 and C_L is 1.2, the equations above can be combined, and the moment can be calculated. In this way the forces and moment were distributed considering Stender approach (Iscol, 2002) and are presented in Table 4.

Table 4. Loads distribution through wing span wise.

Station [mm]	L [daN]	My [daN.mm]
500	847.22	-98842.16
1000	797.87	-93085.18
1500	734.99	-85749.17
2000	656.18	-76554.18
2500	552.78	-64490.64
3000	246.62	-28772.72

In the model each rib was considered as a station and the loads were applied there. In order to apply the forces and moment calculated, a rigid element was used, and its independent node was considered being at 1/4 of the chord, as it can be seen on Figure 5.

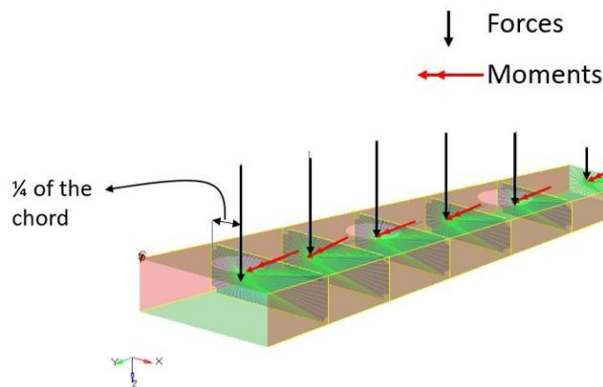


Figure 5. Equivalent forces and moments applied in each station. Adapted from: Santos e tal. (2021).

For the model with high level of detail, the initial condition considers the displacement of the interface nodes between the portioned region and the rest of the wing. The enforced displacement was applied in the model with high level of detail. As the model with such level of detail is more refined than the model with intermediate level of detail, rigid elements are used to connect the point of enforced displacement and the elements of this model. The approach of applying enforced displacement works together with the constraints. Thus, the stiffness matrix is multiplied by the displacement vector to obtain the force vector and consequently the stress field can be calculated..

Results and discussion

Before comparing the stiffness obtained for the fasteners, the critical region to be detailed must be specified. The spanwise shear load distribution through the wing was collected considering the entire wing and it is divided in four regions, as it can be seen on Figure 6. The shear load distribution decreases from the root to the tip of the wing and it can be observed that the corner two is the critical one. In this way, the region near rib 1 of corner 2 was the one used to be detailed and the one to which the aforesaid boundary conditions were applied.

After deciding which region was going to be detailed, the model with high level of detail considering material, geometrical and contact nonlinearity was built, as it was presented in Figure 7. Table 5 shows the statement of the model used to represent the region analyzed.

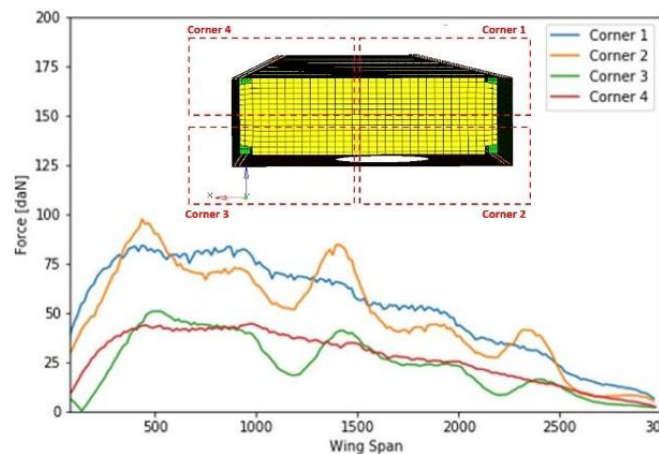


Figure 6. Shear Load for intermediate level of detail.

Table 5. High level of detail model statement.

Type	Number of elements
Nodes	51571
Hexa elements	39075
Penta Elements	656
Rigid Elements	56
SPC	56
Enforced Displacement	56

To calculate the stiffness for model with high level of detail, the relative displacement at the fasteners was obtained and the calculation was performed considering two regions, the top region is at the Spar and the bottom is at the skin. The stiffness calculation is performed only considering a portion of the entire model, as it was described previously. A total of five fasteners were considering at the detailed region and the enforced displacement are applied at the extremity of the model.

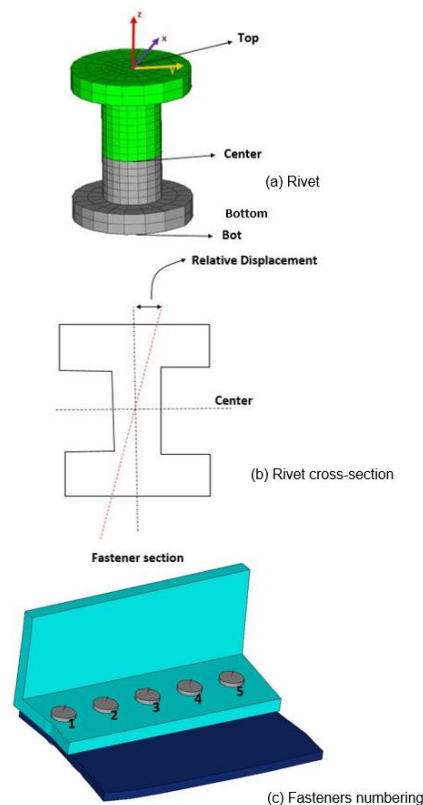


Figure 7. Region choose to be detailed: (a) rivet; (b) rivet cross-section; (c) fasteners numbering.

Translational stiffness was calculated considering the relative displacement obtained in the model with high level of detail. The calculations were performed for the portion of the fastener at the spar region and at the skin region and the results are presented in Figure 8. Those results were calculated considering the displacement at the y direction, which was the critical one. Besides, the forces were obtained considering a freebody at the region of influence at the plate. As it can be noted there are a difference in the translational stiffness considered while using Rutman approach and using a model with high level of detail.

The rotational stiffness was calculated considering the relative rotation of the fastener at each portion, whether spar or skin region and the moment acting in the region were obtained also considering a freebody at the region of the plate influenced by the fastener. Figure 9 presents the comparative between the rotational stiffness obtained from the model with high and intermediate level of detail.



Figure 8. Translational stiffness.

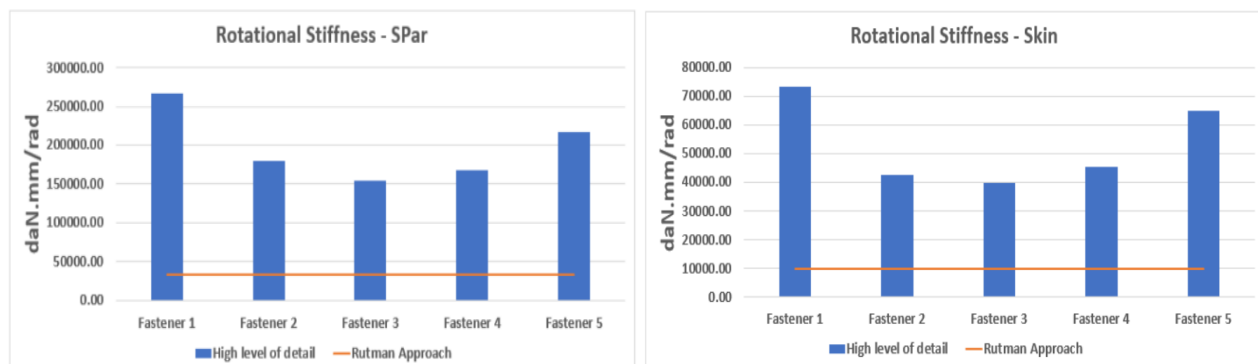


Figure 9. Rotational stiffness at spar.

Conclusion

Some differences in stiffness in joint region were observed by changing from one level of detail to another. These differences are not similar when comparing translational stiffness to rotational stiffness. It is possible to see that the model with high level of detail has large translational stiffness for the fasteners at the extremity and less for the ones at the center, when compared to the Rutman approach (Santos et al., 2021). This behaviour is similar for both regions, whether skin or spar, which means that using the Rutman approach could result in an overall result more flexible for the model.

There were significant differences for stiffness when observing rotational condition. The model with high level of detail presents a larger rotational stiffness when compared to the Rutman approach. This observation can be explained due to the simplification used. Basically the simplification considered does not consider the fastener head and its contact between the plates, which can generate an increase in rotational stiffness. But even with these large differences in rotational stiffness the influence in the shear load is not significant as the effect of translational stiffness.

The use of model with intermediate level of detail has shown safety since the fasteners load distribution are higher than the one obtained for the model with high level of detail. The intermediate model is feasible for the beginning of product development, when the data related to the load distribution and the characteristics of the product are in low maturity and changes in the product and consequently in load distribution are expected all the time.

Most aircraft joints are assembled with rivets, which is easier to assemble and disassemble. Future works can consider other specific methods of connection, like the insertion of adhesive in riveting joint. Zhao et al. (2020) show the positive effects of applying adhesive which makes the joint stronger and with better fatigue properties, better corrosion resistance and also grants the possibility of removing the sealing in operation process.

Acknowledgments

The authors acknowledge the financial supports granted by CNPq (Conselho Nacional de Desenvolvimento Científico e Tecnológico) and FAPEMIG (Fundação de Amparo à Pesquisa do Estado de Minas Gerais).

References

- Abbott, I. H., & von Doenhoff, A. E. (2012). *Theory of wing sections: including a summary of airfoil data*. Courier Corporation.
- Askari, R., Bois, C., & Danoun, A. (2021). Numerical approach to study the effect of shape defect in multi-fastened joints during the assembly process. *CIRP Journal of Manufacturing Science and Technology*, 33, 506-519. DOI: <https://doi.org/10.1016/j.cirpj.2021.05.002>
- Askari, R., Bois, C., & Wagnier, H. (2016). Effect of hole-location error on the strength of fastened multi-material joints. *Procedia CIRP*, 43, 292-296. DOI: <https://doi.org/10.1016/j.procir.2016.02.040>
- Chaves, C. E., & Fernandes, F. F. (2016). A review of aircraft joints design. *Aircraft Engineering and Aerospace technology: an International Journal*, 88(3), 411-419, 2016. DOI: <https://doi.org/10.1108/AEAT-10-2012-0184>
- Gray, P., & McCarthy, C. A. (2011). A highly efficient user-defined finite element for load distribution analysis of large-scale bolted composite structures. *Composites Science and Technology*, 71(12), 1517-1527. DOI: <https://doi.org/10.1016/j.compscitech.2011.06.011>
- Huan, H., & Liu, M. (2017). Effects of squeeze force on static behavior of riveted lap joints. *Advances in Mechanical Engineering*, 9(5), 1687814016686891. DOI: <https://doi.org/10.1177/1687814016686891>
- Huskamuri, M., & Lagdive, H. (2017). Stress analysis of riveted lap joint using finite element method. *Journal NX*, 3(3), 70-74.
- Iscond, P. H. (2002). *Introdução às cargas nas aeronaves*. Belo Horizonte, MG: UFMG.
- Liu, F., Yao, W., Zhao, L., Wu, H., Zhang, X., & Zhang, J. (2020). An improved 2D finite element model for bolt load distribution analysis of composite multi-bolt single-lap joints. *Composite Structures*, 253, 112770. DOI: <https://doi.org/10.1016/j.compstruct.2020.112770>
- Liu, F., Zhang, J., Zhao, L., Xin, A., & Zhou, L. (2015). An analytical joint stiffness model for load transfer analysis in highly torqued multi-bolt composite joints with clearances. *Composite Structures*, 131, 625-636. DOI: <https://doi.org/10.1016/j.compstruct.2015.06.003>
- Niu, M. C. Y. (2011). *Airframe structural design: practical design information and data on aircraft structures* (2nd ed.). Hong Kong Conmilit Press.
- Sadowski, T., Balawender, T., Śliwa, R., Golewski, P., & Kneć, M. (2013). Modern hybrid joints in aerospace: modelling and testing. *Archives of Metallurgy and Materials*, 58, 163-169. DOI: <https://doi.org/10.2478/v10172-012-0168-3>
- Santos, M. T., de Sá Martins, R., & Greco, M. (2021). Mechanical Behavior comparison of aircraft joints modeling Comparação de comportamento mecânico da modelagem de juntas de aeronaves. *Brazilian Journal of Development*, 7(8), 82310-82320. DOI: <https://doi.org/10.34117/bjdv7n8-439>
- Skorupa, M., Machniewicz, T., Korbel, A., & Skorupa, A. (2010). Rivet flexibility and load transmission for a riveted lap joint. *Archive of Mechanical Engineering*, 57(3), 235-245. DOI: <https://doi.org/10.2478/v10180-010-0012-0>
- Verwaerde, R., Guidault, P. -A., & Boucard, P. -A. (2021). A non-linear finite element connector model with friction and plasticity for the simulation of bolted assemblies. *Finite Elements in Analysis and Design*, 195, 103586. DOI: <https://doi.org/10.1016/j.finel.2021.103586>
- Zhao, H., Xi, J., Zheng, K., Shi, Z., Lin, J., Nikbin, K., ... Wang, B. (2020). A review on solid riveting techniques in aircraft assembling. *Manufacturing Review*, 7(40), 1-18. DOI: <https://doi.org/10.1051/mfreview/2020036>